

Production of oleogel from palm olein and rice bran oil in combination with octenyl succinate anhydrous modified porang glucomannan

¹Widarta, I.W.R., ²Rukmini, A., ^{3,*}Raharjo, S., ³Santoso, U. and ³Supriyadi

¹Study Program of Food Technology, Faculty of Agricultural Technology, Udayana University, Bali, Indonesia

²Study Program of Food Technology, Faculty of Science and Technology, Widya Mataram University, Yogyakarta 55281, Indonesia

³Department of Food and Agricultural Product Technology, Faculty of Agricultural Technology, Universitas Gadjah Mada, Bulaksumur, Yogyakarta 55281, Indonesia

Article history:

Received: 22 December 2023

Received in revised form: 15 March 2024

Accepted: 29 April 2024

Available Online: 28 January 2025

Keywords:

Porang glucomannan,
Oleogel,
Palm olein,
Rice bran oil

DOI:

[https://doi.org/10.26656/fr.2017.9\(1\).413](https://doi.org/10.26656/fr.2017.9(1).413)

Abstract

Octenyl succinate anhydrous modified Porang Glucomannan (PGOS) has amphiphilic characteristics so it has the potential to be used as a gelator for oleogel production using the emulsion-template method. The aim of this study was to obtain the appropriate PGOS concentration and oil/water ratio in oleogel production using palm olein and rice bran oil fractions. The concentration of PGOS consists of 1; 2; or 3% while the oil/water ratio consists of 40:60; 45:55; or 50:50. Parameters observed included iodine value and the fatty acid profile of palm olein and rice bran oil, oil loss and emulsion microstructure, oleogel hardness, fourier transform infrared spectroscopy (FTIR) and X-ray diffraction (XRD) profiles. The results showed that the oleogel formed using rice bran oil produced an oleogel with better characteristics than palm olein. PGOS concentration of 1% with an oil/water ratio of 40:60 was able to reduce oil loss to 0%. The oleogel formation occurs because the oil is trapped in a network formed through intermolecular hydrogen bonds which were confirmed from the FTIR and XRD profiles. Oleogel can be applied as a substitute for animal fat in food products.

1. Introduction

Solid fat affects many properties of plastic fat including, structure, texture, mouthfeel, and flavor release in food products (Patel and Dewettinck, 2016; Patel *et al.*, 2020). On the other hand, solid fats contain high levels of saturated fat, which can lead to chronic diseases such as diabetes, obesity, and cardiovascular disease when consumed in excess. FAO/WHO recommends limiting saturated fat consumption to no more than 10% of daily calorie consumption (Oh and Lee, 2018). Many efforts have been made to structure oils rich in unsaturated fatty acids into plastic fats, including interesterification, partial hydrogenation, and fractionation (Ögütçü *et al.*, 2015). Enzymatic interesterification is able to produce a trans-fat-free final product without affecting its sensory properties, but it is very expensive. Meanwhile, partial hydrogenation produces trans fats which have a negative impact on cardiovascular health, and other methods produce final products containing saturated fatty acids (Puscas *et al.*, 2020). One approach that can be taken to produce plastic fat with a high content of unsaturated fatty acids and free

of trans fat is oleogelation.

Oleogelation is a gel system that is formed because the oil liquid is immobilized in a self-assembled network by oleogelator molecules without modifying the chemical characteristics of the oil. Oil systems that are structured through oleogelation are known as oleogels or organogels (Patel and Dewettinck, 2016; Oh and Lee, 2018; Espert *et al.*, 2020). The cost of oil structuring by oleogelation is relatively the same as the conventional crystallization process because it does not require modification of industrial equipment (Stahl *et al.*, 2018).

Oil structuring to produce oleogel can be done by direct dispersion of oleogelator in oil or using an emulsion template (Patel and Dewettinck, 2016). The advantages of using the indirect method (emulsion template) compared to the direct method are that it does not use surfactants and high temperatures (Patel, Cludts, Sintang, Lewille *et al.*, 2014). The indirect method is the most developed approach in recent times. The formation of oleogel begins with the formation of an oil/water emulsion with high-performance homogenization, then

*Corresponding author.

Email: sraharjo@ugm.ac.id

the emulsion is dried in an oven or freeze dryer to form a network that traps oil. The oleogel produced by this method has a high oil binding capacity or low oil loss without changing the fatty acid profile and triglyceride molecules structure, thus maintaining the unsaturated fatty acid content of the oil used (Abdolmaleki *et al.*, 2020; Silva *et al.*, 2021).

The application of hydrocolloids as oleogelators is highly recommended because they are food grade, cheaper, and widely available. Oleogel formation using the emulsion template method generally combines surface active polysaccharides such as hydroxypropyl methyl cellulose (HPMC) or methylcellulose (MC) as an emulsifier with non-surface active polysaccharides such as xanthan gum as a thickening agent. Furthermore, the aqueous phase is evaporated to form a network that physically traps oil in a polysaccharide matrix (Patel, Cludts, Sintang, Lesaffer *et al.*, 2014). The oleogelator requirements are effective in low concentrations, safe, and inexpensive (Espert *et al.*, 2020). Therefore, it is necessary to use a more effective type of oleogelator with a lower amount. An alternative that can be used is to use hydrocolloids which have the natural ability to form a gel. Based on our previous research, octenyl succinate anhydrous modified porang glucomannan (PGOS) has surface active and high viscosity properties so that it can act as a good emulsifier. PGOS is produced by modifying porang glucomannan using 2.25% Na₂CO₃ and 6.19% octenyl succinate anhydride (OSA) in the microwave. The degree of OSA substitution produced is 1.02% and PGOS has an emulsion capacity and stability of 34.6% and 32.5%, respectively (Widarta *et al.*, 2022). PGOS has good emulsion capacity and stability so it has the potential to be used as an oleogelator in the production of oleogels formed by the emulsion template method.

The concentration of oleogelator affects the formation of oleogel. The use of oleogelator with a very low concentration is not sufficient to form a gel network, while too high a concentration will produce a hard solid (Laredo *et al.*, 2011). In addition, the oil/water ratio affects the emulsion stability. The high oil/water ratio results in separation related to the emulsifier's ability (Su *et al.*, 2019). The robustness of the oleogel produced is also influenced by the characteristics of the oil used. The level of unsaturation of fatty acids in the oil also affects the firmness of the oleogel. The oil with a high content of unsaturated fatty acids has the potential to produce a strong oleogel. Oils dominated by unsaturated fatty acids (>50%) both oleic, linoleic and linolenic acids showed greater degrees of conformational freedom. Higher unsaturation of fatty acids causes a higher molar volume of solvent to facilitate the formation of a larger number

of interpolymers junction zones and produce a stronger gel (Gravelle *et al.*, 2016). In addition, high content of long-chain triglycerides will produce a stronger gel at a lower concentration of oleogelator (Cerqueira *et al.*, 2017). This study aimed to obtain the appropriate PGOS concentration and oil/water ratio to obtain an oleogel with low oil loss, as well as evaluate the ability of the palm olein fraction with rice bran oil which has different levels of unsaturation of fatty acids on the formation of oleogel.

2. Materials and methods

2.1 Materials

Octenyl succinic anhydride-modified Porang glucomannan (PGOS) obtained from previous research (Widarta *et al.*, 2022), palm olein ("Tropical"), and rice bran oil ("Oryza Grace") were purchased from a local market. Anhydrous methanol, acetyl chloride, potassium iodide, starch indicator, sodium thiosulfate, and sodium methoxide were purchased from Sigma Chemical Co. (St. Louis, MO).

2.2 Characterization of the fatty acid profile of palm olein and bran oil

The fatty acid profile of palm olein and bran oil was determined in gas chromatography (GC-2010 Shimadzu, Japan) with an FID detector (Gómez-Estaca *et al.*, 2019). A sample of 10 mg was derivatized to fatty acid methyl ester (FAME) using 0.5 M sodium methoxide. GC analysis using 1 µL of FAME which has been extracted with 4 ml of hexane. Separations were carried out in an Agilent DB 23 column (30 m, 0.25 mm id, film thickness 0.25-µm, ref. 122-2332) by split injection (40:1) and helium at a constant flow of 1.2 mL/min. The injector temperature was set at 250°C and the detector temperature at 260°C. The oven temperature profile was 125°C for 1 min, then increased by 8°C/min to 145°C for 26 mins, then increased to 220°C for 5 mins. A standard consisting of 37 fatty acids (Supelco 37 FAME Mix C8-22, USA) is used as a comparison of retention time in the identification process. Margaric acid (C17:0) is used as an internal standard.

2.3 Iodine value

The iodine value was analyzed by the Wijs method (American Oil Chemists' Society [AOCS], 2022).

2.4 Preparation of oleogel

The process of making oleogel was carried out as reported by Patel, Cludts, Sintang, Lewille *et al.* (2014). PGOS (1; 2; 3% w/w of oil) was weighed in a beaker then added water (50; 55; or 60 g), then heated at a temperature of 60°C on a hotplate for 20 mins while

stirring at 400 rpm. The PGOS solution was cooled to room temperature. The oil (40, 45 or 50 g of palm olein or rice bran oil) was then added to the PGOS solution and homogenized with an ultra-turrax homogenizer (T50 Basic IKA WERKE, Germany) at 10,000 rpm for 5 mins. Furthermore, the determination of oil loss and microstructural observations were carried out. The oleogel emulsion which has a low oil loss (physically there is no visible separation of the oil phase in the emulsion) is dried using a freeze dryer for further texture testing.

2.5 Oil loss

Oil loss was determined was carried out as reported by Meng *et al.* (2018a). The oleogel was weighed about 1-1.5 g (m_1) in an Eppendorf tube of known weight, then centrifuged at 4°C, 10000 rpm for 15 mins. The supernatant in the form of loose oil was discarded and the Eppendorf tube was weighed again (m_2). Oil loss is determined by the following equation:

$$\text{Oil loss} = (m_1 - m_2) / m_1 \times 100\% \quad (11)$$

Where m_1 is the weight of the initial sample and m_2 is the weight of the final sample after the supernatant is removed.

2.6 Microstructure

The oleogel microstructure was observed with an OptiLab microscope binocular head (Olympus CX21 LED, US), using a 40× magnification (Espert *et al.*, 2020). The oleogel emulsion sample was dropped on a glass slide and then observed under a microscope.

2.7 Hardness

Samples that have been removed from the freeze dryer are then tested for oleogel hardness. The sample was removed from the cup used during drying and then placed in the center of the Universal Testing Machine (UTM, Zwick, UK) metal plate (Canti *et al.*, 2021). The diameter of the probe used is 12.7 mm, the test speed is 10 mm/min, the pre-load is 0.01 N, the pre-load speed is 300 mm/min, and the standard test is compression.

2.8 Fourier transform infrared spectroscopy

FTIR analysis was carried out using an FTIR spectrometer (Spectrum 100; Thermo Scientific Nicolet iS10, USA) with a wavenumber range of 400-4000 cm^{-1} with a resolution of 8 cm^{-1} (Meng, Li, Liu *et al.*, 2018). PGOS, oleogel, and oil mixed with potassium bromide (1:50), then dried at 105°C for 12 hrs and pressed into tablets for analysis. All spectra were scanned 32 times with background and ATR correction.

2.9 X-ray diffraction analysis

The measurement of polymorphism properties was carried out as reported by Jiang *et al.* (2021). X-ray diffractometer (XRD Rigaku MiniFlex 600, Japan) equipped with a Cu anode and a ceramic x-ray tube was used to identify the polymorphic transformation of the samples at room temperature. PGOS and oleogel were scanned from 4° to 80° (2- θ) in 0.03°/min increments.

2.10 Thermal analysis

The sample was weighed as much as 5 mg in an aluminum container and tightly closed. Sample containers were stored in a refrigerator at 5°C for 24 hrs before testing. The sample containers were then taken directly from the refrigerator (consecutively, one by one) and put into the differential scanning calorimeter (DSC 4000 Pyris 1 Perkin Elmer, USA) and heated from -20°C to 300°C at a rate of 10°C/min, nitrogen gas flow 20 mL/min (Yang *et al.*, 2017).

2.11 Statistical analysis

The analysis was conducted using a completely randomized design. All experimental units were repeated three times. Analysis of variance (ANOVA) was computed using SPSS 16.0. Duncan's Multiple Range Test DMRT was used to determine the significance of differences among experimental mean values ($p < 0.05$).

3. Results and discussion

3.1 The fatty acid profile of palm olein and rice bran oil

The fatty acid profile of palm olein and rice bran oil fractions can be seen in Table 1. The palm olein fraction contains higher saturated fatty acids than rice bran oil. Palm olein and rice bran oil contain high palmitic acid (C16:0) the main saturated fatty acid contained in palm olein and rice bran oil, where the amount of palmitic acid in the palm olein fraction is higher than that of rice bran oil. Furthermore, monounsaturated fatty acids are dominated by oleic acid (C18:1). Meanwhile, the composition of polyunsaturated fatty acids, especially linoleic acid, was higher in rice bran oil than in palm olein. The total saturated fatty acids in palm olein reached 44.23% while the levels of unsaturated fatty acids reached 55.77% (Hashem *et al.*, 2017). Rice bran oil contains high unsaturated fatty acids, dominated by oleic acid and linoleic acid ($\approx 78\%$ w/w), while the saturated fatty acids are dominated by palmitic and stearic acids ($\approx 20\%$ w/w) (Righetti *et al.*, 2019; Benitez *et al.*, 2020). A high content of unsaturated fatty acids is highly desirable in the formation of oleogel. Oils with higher unsaturated fatty acid content form oleogels more easily and produce stronger oleogels (Han *et al.*, 2022).

Table 1. Fatty acid profile of palm olein and rice bran oil.

Fatty acid (FA)	% Fatty acid from the total of fatty acid	
	Palm olein	Rice bran oil
Lauric acid (C12:0)	0.15	0.00
Myristic acid (C14:0)	0.95	0.46
Pentadecanoic acid (C15:0)	0.05	0.02
Palmitic acid (C16:0)	36.00	20.17
Stearic acid (C18:0)	4.32	2.50
Arachidic acid (C20:0)	0.42	1.10
Behenic acid (C22:0)	0.24	0.42
Total Saturated FA	42.12	24.66
Palmitoleic acid (C16:1)	0.18	0.18
Cis-9-oleic acid (C18:1)	43.85	43.03
Eicosenoic acid (C20:1)	0.18	0.59
Erucid acid (C22:1)	0.02	0.09
Total MUFA	44.23	43.90
Linoleic acid (C18:2)	13.17	34.95
Linolenic acid (C18:3)	0.18	1.13
Total PUFA	13.35	36.07

3.2 Iodine value of palm olein and rice bran oil

The iodine value of rice bran oil is higher than that of palm olein, where the iodine value of rice bran oil is 95.05 g I₂/100 g, while the iodine value of palm olein is 63.33 g I₂/100 g. The iodine number shows the level of unsaturation of fatty acids or the average number of double bonds in fatty acids. The higher the iodine number, the higher the level of unsaturation (Phan *et al.*, 2021). The iodine number correlates with the fatty acid profile, where the levels of unsaturated fatty acids are higher in rice bran oil than in palm olein. The iodine value in the palm olein fraction corresponds to the super olein iodine value of around 60.8-64.8 (Hashem *et al.*, 2017). The super olein has an iodine value greater than 60, which is 65.4 g I₂/100 g (Mello *et al.*, 2021). The iodine value of rice bran oil ranged from 90-105 g I₂/100 g (Kusum *et al.*, 2011) or 100.15 to 105.09 g I₂/100 g (Phan *et al.*, 2021). The difference in iodine number in rice bran oil can be influenced by the method and conditions of extraction (Juchen *et al.*, 2019; Phan *et al.*, 2021; Xu *et al.*, 2021).

3.3 Palm olein oleogel

3.3.1 Oil loss

The oleogel is produced using an indirect method in which the emulsion template is prepared in an oil-in-water system. Oleogel in the form of an oil-in-water emulsion is then determined for the oil loss. ANOVA showed that the interaction between the concentration of PGOS (C1, C2, C3) and the oil/water ratio (R1, R2, R3) had a very significant effect on oil loss in the oleogel

emulsion (Figure 1). The lowest oil loss was obtained in the treatment of 3% PGOS concentration with an oil/water ratio of 40:45 and 45:55 which were not significantly different from the 2% PGOS concentration. Meanwhile, the highest oil loss was obtained at 1% PGOS concentration which was not significantly different from the 2% concentration at a 50:50 oil/water ratio. The higher the PGOS concentration, the lower the oil loss, but the higher the oil/water ratio, the higher the oil loss. The higher ratio of oil to water resulted in the weakening of the ability of PGOS as an oleogelator. The higher the ratio of oil to water, the more separated the emulsion formed (Su *et al.*, 2019).

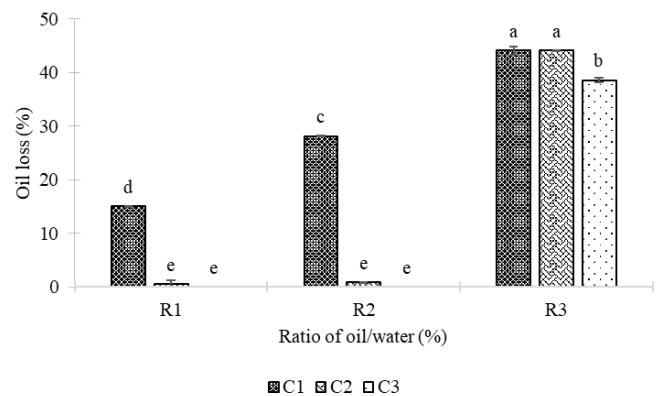


Figure 1. The relationship between PGOS concentrations (C1, C2, C3 are 1, 2, 3 %, respectively) and the palm olein/water ratio (R1, R2, R3 are 40:60, 45:55, and 50:50, respectively) to the percentage of oil loss. Bars with different notations are statistically significantly different ($p < 0.05$).

The increasing concentration of HPMC in the production of oleogels by the indirect method (emulsion-template) will result in more stable emulsions, more compact networks, higher gel strength, and better oil loss (Meng *et al.*, 2018b). The lower emulsifier concentration caused the emulsification process to be less efficient. In addition, the oil-water ratio is a factor that affects the stability and droplet size of the emulsion. The high amount of oil causes less oil to be trapped by the emulsifier, resulting in weak emulsions and larger droplet sizes (Kori *et al.*, 2021).

3.3.2 Microstructure of palm olein oleogel emulsion

The results of the observation of the microstructure of the oleogel emulsion can be seen in Figure 2. Based on the oil loss data, it can be seen that the oleogel which produces higher oil loss has a larger droplet size than the oleogel which has lower oil loss. This indicates the occurrence of coalescence between oil droplets which causes increased oil loss. Coalescence occurs because PGOS is not able to wrap oil droplets well so they combine to form larger droplet sizes (Meng, Li, Liu *et al.*, 2018). Emulsions with larger droplet sizes tend to have low emulsion stability (Phan *et al.*, 2021). The

higher saturated fatty acid content causes larger droplet sizes in palm olein resulting in lower emulsion stability (Zheng *et al.*, 2021).

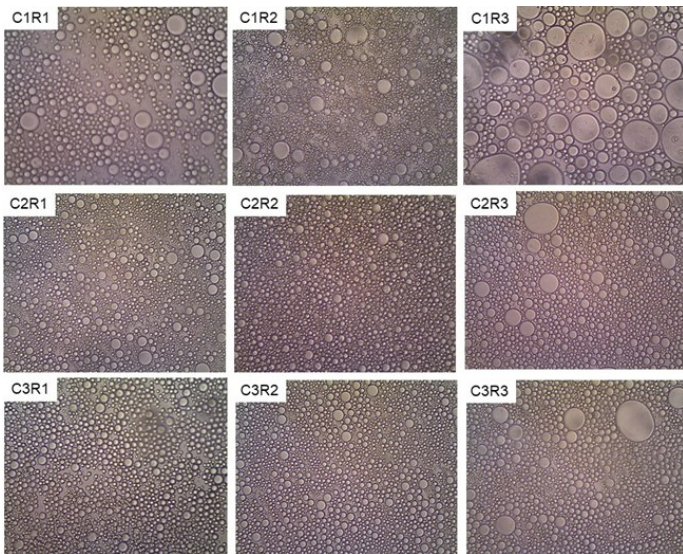


Figure 2. The relationship between PGOS concentrations (C1, C2, C3 are 1, 2, 3 %, respectively) and the oil/water ratio (R1, R2, R3 are 40:60, 45:55, and 50:50, respectively) to the microstructure of palm olein oleogel emulsion.

The higher the PGOS concentration, the smaller the oil droplet size and the lower the oil loss. The higher the amount of surfactant added, the more stable the emulsion produced (Meng *et al.*, 2018b). The increasing surfactant concentration resulted in a decrease in emulsion droplet size so that more surface covered the interfacial area at the same mass/volume of oil and resulted in a more stable emulsion (Hadi *et al.*, 2020).

3.3.3 Hardness

Hardness measurements were carried out after the oleogel emulsion was dried with a freeze-dryer. This is because measuring the texture of the emulsion is difficult to do. Hardness measurements were only carried out on samples with the category of no separation of oil in the oleogel emulsion. The results of hardness measurements can be seen in Figure 3 and the dried oleogel can be seen in Figure 4.

Figure 3 shows that increasing the concentration of added PGOS increased the hardness of the oleogel and an increase in the ratio of oil to water resulted in a slight decrease in hardness. The higher the addition of oleogelator, the resulting oleogel became harder and had higher oil binding capacity (Stahl *et al.*, 2018). The increase in hardness is positively correlated with the results of observations of the oleogel microstructure. The smaller the oil droplet size, the higher the hardness produced. The increase in oleogelator resulted in a more compact and tougher tissue structure and smaller tissue holes so that more oil was bound in it without even being released (Meng *et al.*, 2018b).

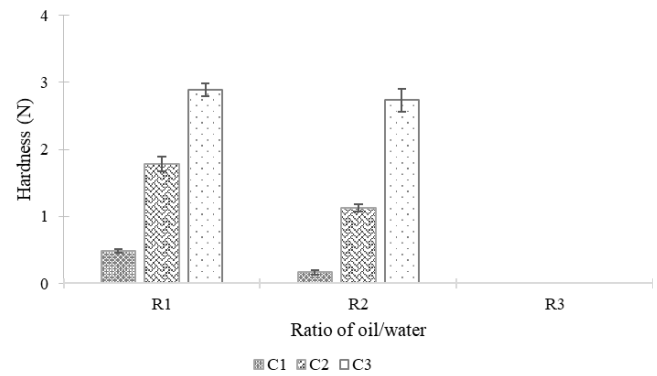


Figure 3. The relationship between PGOS concentrations (C1, C2, C3 are 1, 2, 3 %, respectively) and the oil/water ratio (R1, R2, R3 are 40:60, 45:55, and 50:50, respectively) to the hardness of palm olein oleogel after lyophilization.

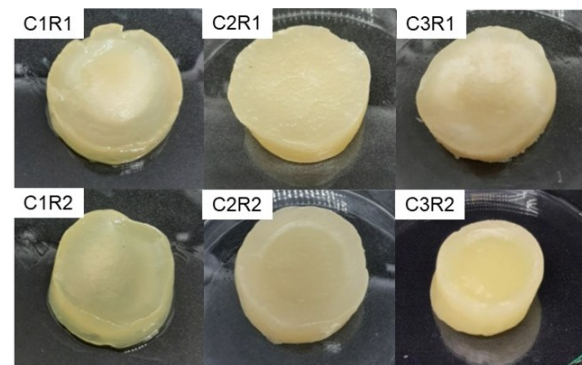


Figure 4. Palm olein oleogel with PGOS as oleogelator after lyophilization. C1, C2, C3 are 1; 2; 3% PGOS concentrations, respectively and R1, R2, R3 are the oil/water ratio of 40:60, 45:55, and 50:50, respectively.

3.4 Rice bran oil oleogel

3.4.1 Oil loss

ANOVA showed that the interaction between the concentration of PGOS (C1, C2, C3) and the oil/water ratio (R1, R2, R3) had a very significant effect on the oil loss of the oleogel emulsion of rice bran oil. The highest oil loss was obtained at a 1% PGOS concentration with an oil/water ratio of 50:50, while the lowest oil loss was obtained at a 1% PGOS concentration with an oil/water ratio of 40:60 which was not significantly different from a 45:55 ratio and a PGOS concentration of 2-3% with oil to water ratio of 40:60, 45:55 and 50:50. The relationship between the concentration of PGOS and the ratio of oil/water to the percentage of oil loss of oleogel can be seen in Figure 5.

The high oil loss in the oleogel formed with 1% PGOS at an oil/water ratio of 50:50 was caused by the insufficient amount of PGOS added to interact with the oil and form a stable emulsion. This can be seen in the larger droplet size when observing the microstructure of the oleogel emulsion. At low emulsifier concentrations, the interaction between droplets weakens, thereby reducing the stability of the emulsion (Bendjaballah *et*

al., 2010). The low amount of emulsifier causes the emulsifier to be not well absorbed by the particle surface so that the particles lose repulsion and attraction in the same proportion. Particles containing different hydrophilic and hydrophobic groups cause a tendency towards one phase (water or oil). Particles that absorb more hydrophilic emulsifiers will tend to repel oil, and vice versa. This instability causes the particles to flocculate and coalesce (Nawangasasi *et al.*, 2018). The higher the ratio of oil to water, the more separated the emulsion formed, this was due to the insufficient ability of the emulsifier to form a stable emulsion (Su *et al.*, 2019).

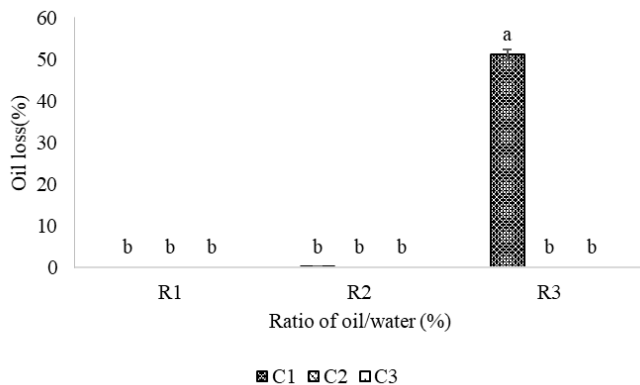


Figure 5. The relationship between PGOS concentrations (C1, C2, C3 are 1, 2, 3%, respectively) and the oil/water ratio (R1, R2, R3 are 40:60, 45:55, and 50:50, respectively) to the percentage of oil loss oleogel. Bars with different notations are statistically significantly different ($p < 0.05$).

Based on oil loss data, rice bran oil has a better emulsion-forming ability than palm olein. This could be due to rice bran oil containing more unsaturated fatty acids and longer chain fatty acids than palm olein. The unsaturated fatty acids and long-chain (C13-18) unsaturated fatty acids in soybean oil caused the particles in the emulsion to repel each other and increase the strength of attraction so that the stability of the emulsion increased. The characteristics of fatty acids such as the size of the polar heads and the charge carried by the fatty acids, and the accumulation of fatty acid chains at the oil-water interface affect the stability of the emulsion (Zheng *et al.*, 2021).

3.4.2 Microstructure of rice bran oil oleogel emulsion

The microstructure of the bran oil oleogel can be seen in Figure 6. Based on the oil loss data, it can be seen that the oleogel that produced a higher oil loss (C1R3) had a larger droplet size than the oleogel which had a lower oil loss. This indicates the occurrence of coalescence between oil droplets which causes increased oil loss. Coalescence is an irreversible process that occurs when small droplets combine to form larger

droplets (Meng *et al.*, 2018b). Emulsions with larger droplet sizes tend to have low emulsion stability. The small droplet size was able to prevent coalescence and Ostwald ripening to produce a stable emulsion (Bendjaballah *et al.*, 2010).

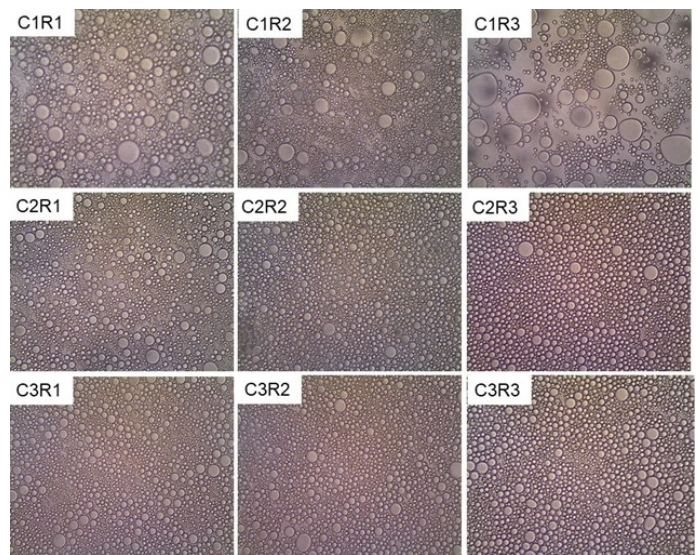


Figure 6. The relationship between PGOS concentrations (C1, C2, C3 are 1, 2, 3 %, respectively) and the oil/water ratio (R1, R2, R3 are 40:60, 45:55, and 50:50, respectively) to the microstructure of rice bran oil oleogel emulsion.

The higher the concentration of PGOS, the droplet size becomes smaller and denser. Increasing the concentration of the emulsifier can reduce the droplet size of the emulsion thereby increasing the stability of the emulsion. The ability to form an emulsion of rice bran oil is better than palm olein because rice bran oil contains more polyunsaturated fatty acids and long-chain fatty acids (Akbari and Nour, 2018). Soybean oil containing more polyunsaturated fatty acids and long-chain fatty acids was able to produce smaller droplet sizes resulting in better emulsion stability. Medium-chain fatty acids (C8:0-C12:0) and monounsaturated fatty acids were not able to resist coalescence and delamination of the emulsion (Zheng *et al.*, 2021).

3.4.3 Hardness

Hardness measurements were also carried out on samples that showed no separation of oil in the oleogel emulsion. The results of the oleogel hardness test can be seen in Figure 7 and Figure 8 shows the lyophilized oleogel. Figure 7 shows that the increase in PGOS concentration and the oil/water ratio increased oleogel hardness. This indicates that the ability of rice bran oil to produce a firm oleogel is better than palm olein. At concentrations of PGOS higher than 1%, the texture tends to be harder. Likewise, higher oil ratios, especially at oil ratios of 45:55 and 50:50 at concentrations of 2% and 3% PGOS resulted in a harder texture than the ratio of 40:60. This indicates that the PGOS concentration and

the oil/water ratio greatly affect the texture of the oleogel produced. The high oil/water ratio can be stabilized by the concentration of PGOS used. The gelator concentration affected the texture, rheology, and oil binding capacity of oleogels. Increasing the concentration of the gelator used (methylcellulose or HPMC) will produce a harder oleogel with higher mechanical strength which is associated with a more stable system with increased oil binding capacity (reduced oil loss) (Espert *et al.*, 2020).

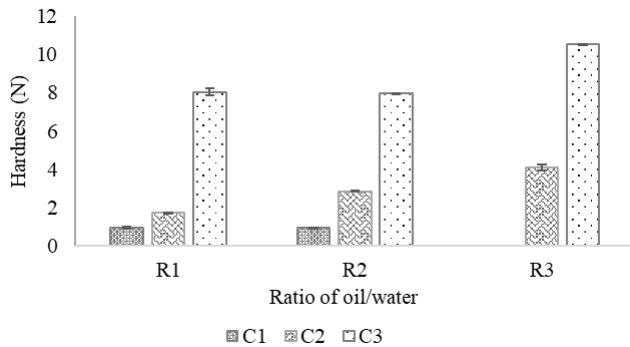


Figure 7. The relationship between PGOS concentrations (C1, C2, C3 are 1, 2, 3 %, respectively) and the oil/water ratio (R1, R2, R3 are 40:60, 45:55, and 50:50, respectively) to the percentage of oil loss oleogel.

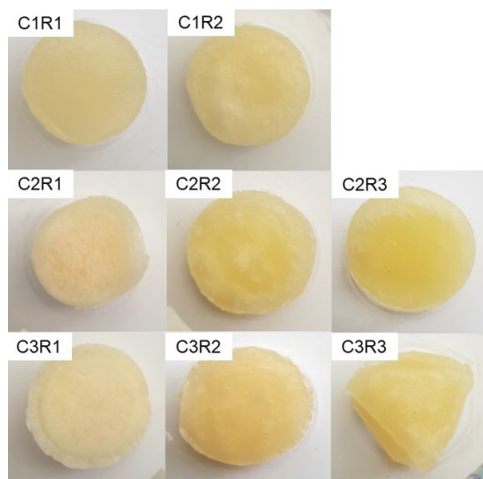


Figure 8. Rice bran oil oleogel with PGOS as oleogelator after lyophilization. C1, C2, C3 are 1; 2; 3% PGOS concentrations, respectively and R1, R2, R3 are the oil/water ratio of 40:60, 45:55, and 50:50, respectively.

Based on the oil loss data, it can be seen that the oleogel produced using rice bran oil is better than using palm olein. PGOS concentration of 1% and oil/water ratio of 40:60 was chosen as the best treatment because in addition to having a low oil loss value, the amount of PGOS used was the least compared to other treatments so that it was more efficient and economical. Therefore, the oleogel produced from 1% PGOS and the oil/water ratio of 40:60 (C1R1) was further characterized including, functional group analysis by FTIR, polymorphism by XRD, and thermal properties by DSC.

3.5 Fourier transformed infrared profile

The results of the FTIR profile of rice bran oil (RBO), bran oil oleogel, and PGOS can be seen in Figure 9. Figure 9 shows that the spectra of rice bran oil are similar to those of oleogel because oleogel is formed by an emulsion of rice bran oil which is freeze-dried. There is a stretching vibration of the O-H group of methyl in PGOS and oleogel indicated by a peak at $3422\text{-}3424\text{ cm}^{-1}$. The strong vibration at the peak indicates the presence of a hydroxyl group (-OH) polysaccharide (Jian *et al.*, 2015; Jiang *et al.*, 2021). There was a shift in peak from 3422 cm^{-1} to 3424 cm^{-1} indicating an intermolecular interaction through the formation of hydrogen bonds and the peak intensity in the oleogel was higher than that of PGOS. This indicates that the hydrogen bonds formed are more intense and the interactions are more complex after the oleogel formation. The intermolecular hydrogen bonds can be formed in the gel system (Sun *et al.*, 2021).

The peak of 3467 cm^{-1} in rice bran oil indicates the presence of intermolecular hydrogen bonds between sitosterol and oryzanol (Puscas *et al.*, 2021). The presence of intermolecular hydrogen bonds in bran oil-based oleogels which were seen at the peak of the band around $3215\text{-}3520\text{ cm}^{-1}$ indicated as β -sitosterol and γ -oryzanol (Sahu *et al.*, 2020). Oleogels with semicrystalline structures can be formed through the binding of oil to polysaccharides which is stabilized by intramolecular or intermolecular hydrogen bonds between polysaccharides (Patel and Dewettinck, 2016; Meng *et al.*, 2018a).

The peak of 3008 cm^{-1} observed in rice bran oil and oleogel is the strain $=\text{C-H}$ in rice bran oil. This shows that oleogel has similar characteristics to rice bran oil, which is that it contains unsaturated fatty acids. Rice bran oil is one type of oil that is rich in monounsaturated fatty acids and polyunsaturated fatty acids. The same peak was also observed in soybean oil rich in unsaturated fatty acids (Meng *et al.*, 2018a; Jiang *et al.*, 2021). The peak of 2925 cm^{-1} was the vibration of methyl (CH_3) which was found in rice bran oil, oleogel, and PGOS. The same was found in soybean oil and KGM (Jian *et al.*, 2015; Meng *et al.*, 2018a; Jiang *et al.*, 2021). The peak of 2854 cm^{-1} is the CH_2 vibration in rice bran oil, such as that found in soybean oil (Jian *et al.*, 2015; Jiang *et al.*, 2021).

Figure 9 also show the presence of a carbonyl group in rice bran oil and oleogel which is seen at the peak of 1746 cm^{-1} , while in PGOS it is seen at 1734 cm^{-1} . The absorption peaks at $1735\text{-}1750\text{ cm}^{-1}$ indicating the presence of a C=O carbonyl group (Fayaz *et al.*, 2017). The presence of a carbonyl group on KGOS seen at 1732 cm^{-1} (Meng, Li, Liu *et al.*, 2018). The presence of this

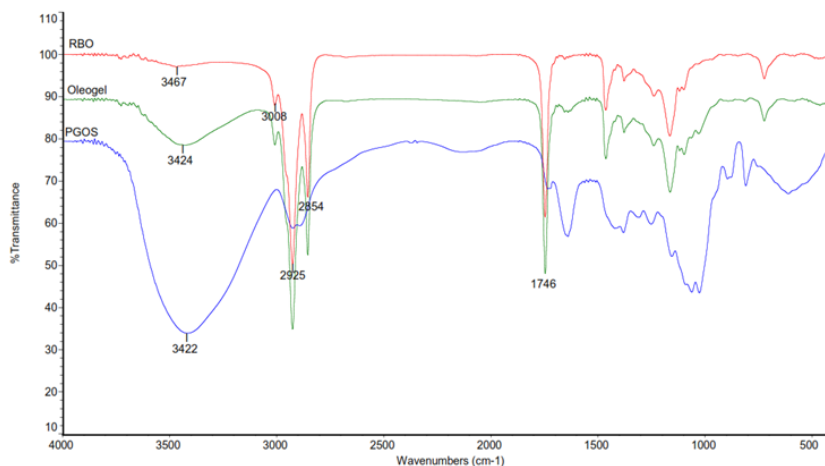


Figure 9. FTIR chromatogram of rice bran oil/RBO (red line), bran oil oleogel (green line), and PGOS (blue line).

carbonyl group in the oleogel is caused by the fatty acids in the rice bran oil and PGOS which is used as a gelator.

3.6 The polymorphism of oleogel and porang glucomannan

Figure 10 shows the semi-crystalline structure (amorphous and crystalline) in both PGOS and oleogel. HPMC powder and xanthan gum as oleogelator also showed semi-crystalline properties (Jiang *et al.*, 2021). Two PGOS diffraction peaks were seen at 19.78° and 36.12° (2θ angle), while the oleogel was seen at 10.34° and 19.80° . This indicates that there is the same peak between PGOS and oleogel, which is around 19.78° - 19.80° , only that the intensity of oleogel is lower than that of PGOS. The same peak indicates no change in the crystalline type (Jiang *et al.*, 2021). The same peak was observed in both HPMC and oleogel which was around 20° (Meng *et al.*, 2018a; Jiang *et al.*, 2021).

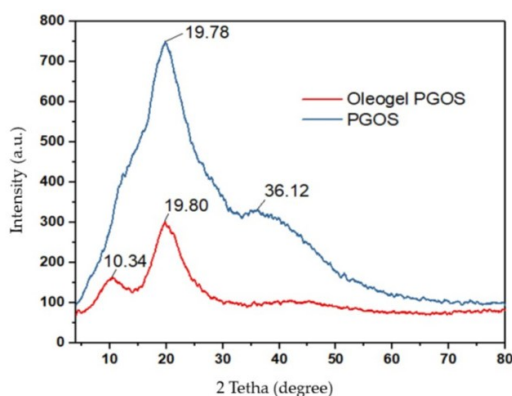


Figure 10. X-ray diffraction (XRD) pattern of rice bran oil oleogel and PGOS.

The peak intensity of oleogel was lower than that of PGOS due to the addition of rice bran oil with liquid characteristics as raw material for oleogel. The crystallinity decreased with increasing water content (Kong *et al.*, 2015). Changes in PGOS crystallization during the formation and lyophilization of the oleogel resulted in a new peak at 10.34° due to the interaction between PGOS molecules through hydrogen bonds. The oleogelator molecules interact in the emulsion solution

mainly through hydrogen bonding resulting in changes in the molecular structure to form an interconnected 3-D network after freeze drying, further trapping the oil to form the oleogel (Jiang *et al.*, 2021). This was confirmed by the results of FTIR analysis which showed a shift and peak intensity between the oleogel and PGOS at 3422 cm^{-1} and 3424 cm^{-1} . In oleogel formation, intermolecular or intramolecular hydrogen bonds between polysaccharides contribute to the formation of the semi-crystalline structure of the oleogel (Meng *et al.*, 2018a). The polysaccharides form a protective layer around the oil droplets in the emulsion and during drying tend to interact with each other to form a regular structure that coats the oil (Meng *et al.*, 2018b).

3.7 Thermal properties of the oleogel and porang glucomannan

DSC analysis was carried out to determine the thermal behavior of oleogel and PGOS both at melting point and crystallization (Puscas *et al.*, 2021). The thermal profile of rice bran oil oleogel and PGOS can be seen in Figure 11. PGOS shows one endothermic peak while the oleogel shows two endothermic peaks. The peak of PGOS melting is seen at a temperature of 87.81°C . Glucomannan with a higher molecular weight has a higher thermal stability, but this is also influenced by its structure and chemical composition. The XRD profile also shows PGOS crystallinity with a higher

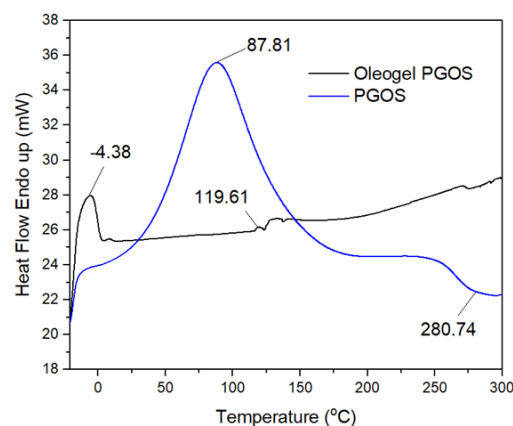


Figure 11. Thermal profile of rice bran oil oleogel and PGOS.

intensity than oleogel. The correlation between molecular structure and thermal behavior is seen when depolymerization occurs through the breaking of glycosidic bonds, there are differences in the thermal behavior of disaccharides and polymeric carbohydrates, where glycosidic bonds between glucose are the most resistant. Therefore, the order of glucose and mannose units in the structural framework can also affect the thermal stability of the glucomannan polymer (Morianan *et al.*, 2014).

The initial melting of oleogel occurs at a temperature of -4.38°C due to rice bran oil as the raw material for oleogel which has a high content of unsaturated fatty acids, especially polyunsaturated fatty acids. This is also confirmed by the presence of the =C-H functional group in the oleogel FTIR profile at peak 3008 cm⁻¹. Subsequent melting occurred at a temperature of 119.61°C due to the addition of oleogelator (PGOS) and intermolecular hydrogen bonds formed on the oleogel as seen in the FTIR and XRD analysis. The type of oil affected the crystallization properties. Oils with saturated fatty acid content melt profile at higher temperatures. The concentration of oleogelator also causes different thermal stability. The length of the triglyceride chain also causes an increase in the crystallization temperature which indicates the formation of a stronger crystal network (Puscas *et al.*, 2021). Mixing two or more substances in various proportions causes a change in melting temperature compared to the pure components (Kim *et al.*, 2022).

4. Conclusion

The PGOS concentration and the oil/water ratio had a significant effect ($p < 0.05$) on the oil loss of the oleogel emulsion. Rice bran oil which is rich in polyunsaturated fatty acids can form oleogel with lower oil loss than the palm olein fraction. The higher the PGOS concentration, the lower the oil loss, while the higher the oil/water ratio, the higher the resulting oil loss. The best treatment was obtained at 1% PGOS concentration and a 40:60 ratio of rice bran oil/water. FTIR and XRD showed that the oleogel was formed because the oil was trapped in the network formed through intermolecular hydrogen bonds. This affects the thermal properties of the oleogel observed from the DSC analysis. The oleogel produced in this study can be used as a substitute for animal fat in food products.

Conflict of interest

The authors declare no conflict of interest.

Acknowledgements

This research was funded by the Ministry of Education, Culture, Research and Technology, Republic of Indonesia grant number 111/E4.1/AK.04.PT/2021.

References

- Abdolmaleki, K., Alizadeh, L., Nayebzadeh, K., Hosseini, S.M. and Shahin, R. (2020). Oleogel production based on binary and ternary mixtures of sodium caseinate, xanthan gum, and guar gum: Optimization of hydrocolloids concentration and drying method. *Journal of Texture Studies*, 51(2), 290-299. <https://doi.org/10.1111/jtxs.12469>
- Akbari, S. and Nour, A.H. (2018). Emulsion types, stability mechanisms and rheology: A review. *International Journal of Innovative Research and Scientific Studies*, 1(1), 11-17. <https://doi.org/10.53894/ijirss.v1i1.4>
- American Oil Chemists' Society (AOCS). (2022). Official methods and recommended practices of the American Oil Chemists' Society, 7th ed. Washington DC: AOCS Press.
- Bendjaballah, M., Canselier, J.P. and Oumeddour, R. (2010). Optimization of oil-in-water emulsion stability: Experimental design, multiple light scattering, and acoustic attenuation spectroscopy. *Journal of Dispersion Science and Technology*, 31(9), 1260-1272. <https://doi.org/10.1080/01932690903224888>
- Benitez, L.O., Castagnini, J.M., Añón, M.C. and Salgado, P.R. (2020). Development of oil-in-water emulsions based on rice bran oil and soybean meal as the basis of food products able to be included in ketogenic diets. *LWT-Food Science and Technology*, 118, 108809. <https://doi.org/10.1016/j.lwt.2019.108809>
- Canti, M., Murdiati, A., Naruki, S. and Supriyanto. (2021). Quality characteristics of chicken sausages using a combination of jack bean. *Food Research*, 5 (3), 249-261. [https://doi.org/10.26656/fr.2017.5\(3\).544](https://doi.org/10.26656/fr.2017.5(3).544)
- Cerqueira, M.A., Fasolin, L.H., Picone, C.S.F., Pastrana, L.M., Cunha, R.L. and Vicente, A.A. (2017). Structural and mechanical properties of organogels: Role of oil and gelator molecular structure. *Food Research International*, 96, 161-170. <https://doi.org/10.1016/j.foodres.2017.03.021>
- Espert, M., Salvador, A. and Sanz, T. (2020). Cellulose ether oleogels obtained by emulsion-templated approach without additional thickeners. *Food Hydrocolloids*, 109, 106085. <https://doi.org/10.1016/j.foodhyd.2020.106085>
- Fayaz, G., Goli, S.A.H. and Kadivar, M. (2017). A novel propolis wax-based organogel: effect of oil type on its

- formation, crystal structure and thermal properties. *Journal of the American Oil Chemists' Society*, 94(1), 47-55. <https://doi.org/10.1007/s11746-016-2915-5>
- Gómez-Estaca, J., Herrero, A.M., Herranz, B., Álvarez, M.D., Jiménez-Colmenero, F. and Cofrades, S. (2019). Characterization of ethyl cellulose and beeswax oleogels and their suitability as fat replacers in healthier lipid pâtés development. *Food Hydrocolloids*, 87, 960-969. <https://doi.org/10.1016/j.foodhyd.2018.09.029>
- Gravelle, A.J., Davidovich-Pinhas, M., Zetzl, A.K., Barbut, S. and Marangoni, A.G. (2016). Influence of solvent quality on the mechanical strength of ethylcellulose oleogels. *Carbohydrate Polymers*, 135, 169-179. <https://doi.org/10.1016/j.carbpol.2015.08.050>
- Hadi, A.N., Marefati, A., Matos, M., Wiege, B. and Rayner, M. (2020). Characterization and stability of short-chain fatty acids modified starch pickering emulsions. *Carbohydrate Polymers*, 240, 116264. <https://doi.org/10.1016/j.carbpol.2020.116264>
- Han, W., Chai, X., Liu, Y., Xu, Y. and Tan, C. (2022). Crystal network structure and stability of beeswax-based oleogels with different polyunsaturated fatty acid oils. *Food Chemistry*, 381, 131745. <https://doi.org/10.1016/j.foodchem.2021.131745>
- Hashem, H.A., Shahat, M., El-Beairy, S.A. and Sabry, A. (2017). Use of Palm Olein for Improving the Quality Properties and Oxidative Stability of Some Vegetable Oils during Frying Process. *Middle East Journal of Applied Sciences*, 7(1), 68-79.
- Jian, W., Siu, K.C. and Wu, J.Y. (2015). Effects of pH and temperature on colloidal properties and molecular characteristics of Konjac glucomannan. *Carbohydrate Polymers*, 134, 285-292. <https://doi.org/10.1016/j.carbpol.2015.07.050>
- Jiang, Q., Du, L., Li, S., Liu, Y. and Meng, Z. (2021). Polysaccharide-stabilized aqueous foams to fabricate highly oil-absorbing cryogels: Application and formation process for preparation of edible oleogels. *Food Hydrocolloids*, 120, 106901. <https://doi.org/10.1016/j.foodhyd.2021.106901>
- Juchen, P.T., Araujo, M.N., Hamerski, F., Corazza, M.L. and Voll, F.A.P. (2019). Extraction of parboiled rice bran oil with supercritical CO₂ and ethanol as co-solvent: Kinetics and characterization. *Industrial Crops and Products*, 139, 111506. <https://doi.org/10.1016/j.indcrop.2019.111506>
- Kim, M., Hwang, H.S., Jeong, S. and Lee, S. (2022). Utilization of oleogels with binary oleogelator blends for filling creams low in saturated fat. *Lwt-Food Science and Technology*, 155, 112972. <https://doi.org/10.1016/j.lwt.2021.112972>
- Kong, X., Qiu, D., Ye, X., Bao, J., Sui, Z., Fan, J. and Xiang, W. (2015). Physicochemical and crystalline properties of heat-moisture-treated rice starch: Combined effects of moisture and duration of heating. *Journal of the Science of Food and Agriculture*, 95 (14), 2874-2879. <https://doi.org/10.1002/jsfa.7028>
- Kori, A.H., Mahesar, S.A., Sherazi, S.T.H., Khatri, U.A., Laghari, Z.H. and Panhwar, T. (2021). Effect of process parameters on emulsion stability and droplet size of pomegranate oil-in-water. *Grasas y Aceites*, 72 (2), e410. <https://doi.org/10.3989/GYA.0219201>
- Kusum, R., Bommayya, H., Fayaz, P.P. and Ramachandran, H. (2011). Palm oil and rice bran oil: Current status and future prospects. *International Journal of Plant Physiology and Biochemistry*, 3(8), 125-132.
- Laredo, T., Barbut, S. and Marangoni, A.G. (2011). Molecular interactions of polymer oleogelation. *Soft Matter*, 7(6), 2734-2743. <https://doi.org/10.1039/c0sm00885k>
- Mello, N.A., Ribeiro, A.P.B. and Bicas, J.L. (2021). Delaying crystallization in single fractionated palm olein with limonene addition. *Food Research International*, 145, 110387. <https://doi.org/10.1016/j.foodres.2021.110387>
- Meng, Z., Qi, K., Guo, Y., Wang, Y. and Liu, Y. (2018a). Effects of thickening agents on the formation and properties of edible oleogels based on hydroxypropyl methyl cellulose. *Food Chemistry*, 246, 137-149. <https://doi.org/10.1016/j.foodchem.2017.10.154>
- Meng, F.B., Li, Y.C., Liu, D.Y., Zhong, G. and Guo, X.Q. (2018). The characteristics of konjac glucomannan octenyl succinate (KGOS) prepared with different substitution rates. *Carbohydrate Polymers*, 181, 1078-1085. <https://doi.org/10.1016/j.carbpol.2017.11.040>
- Meng, Z., Qi, K., Guo, Y., Wang, Y. and Liu, Y. (2018b). Macro-micro structure characterization and molecular properties of emulsion-templated polysaccharide oleogels. *Food Hydrocolloids*, 77, 17-29. <https://doi.org/10.1016/j.foodhyd.2017.09.006>
- Moriana, R., Zhang, Y., Mischnick, P., Li, J. and Ek, M. (2014). Thermal degradation behavior and kinetic analysis of spruce glucomannan and its methylated derivatives. *Carbohydrate Polymers*, 106(1), 60-70. <https://doi.org/10.1016/j.carbpol.2014.01.086>
- Nawangasasi, I.R., Pramono, Y.B., Hintono, A. and Paramita, V. (2018). Water-in-oil-in-water (W/O/W) double emulsion morphology and its degradation on instant noodle seasoning. *Agritech*, 38(2), 151-159. <https://doi.org/10.22146/agritech.27550>
- Oh, I.K. and Lee, S. (2018). Utilization of foam structured hydroxypropyl methylcellulose for oleogels and their application as a solid fat replacer in muffins. *Food*

- Hydrocolloids*, 77, 796-802. <https://doi.org/10.1016/j.foodhyd.2017.11.022>
- Ögütçü, M., Yılmaz, E. and Güneşer, O. (2015). Influence of storage on physicochemical and volatile features of enriched and aromatized wax organogels. *Journal of the American Oil Chemists' Society*, 92(10), 1429-1443. <https://doi.org/10.1007/s11746-015-2719-z>
- Patel, A.R., Cludts, N., Sintang, M.D., Lewille, B., Lesaffer, A. and Dewettinck, K. (2014). Polysaccharide-based oleogels prepared with an emulsion-templated approach. *A European Journal of Chemical Physics and Physical Chemistry*, 15(16), 3435-3439. <https://doi.org/10.1039/c4fo00624k>
- Patel, A.R., Cludts, N., Sintang, M.D., Lesaffer, A. and Dewettinck, K. (2014). Edible oleogels based on water soluble food polymers: Preparation, characterization and potential application. *Food and Function*, 5(11), 2833-2841. <https://doi.org/10.1039/C4FO00624K>
- Patel, A.R. and Dewettinck, K. (2016). Edible oil structuring: An overview and recent updates. *Food and Function*, 7(1), 20-29. <https://doi.org/10.1039/c5fo01006c>
- Patel, A.R., Nicholson, R.A. and Marangoni, A.G. (2020). Applications of fat mimetics for the replacement of saturated and hydrogenated fat in food products. *Current Opinion in Food Science*, 33, 61-68. <https://doi.org/10.1016/j.cofs.2019.12.008>
- Phan, V.M., Tran, H.C. and Sombatpraiwan, S. (2021). Rice bran oil extraction with mixtures of ethanol and hexane. *Songklanakarin Journal of Science and Technology*, 43(3), 630-637.
- Puscas, A., Muresan, V., Socaciu, C. and Muste, S. (2020). Oleogels in food: A review of current and potential applications. *Foods*, 9(1), 70. <https://doi.org/10.3390/foods9010070>
- Puscas, A., Mureşan, V. and Muste, S. (2021). Application of analytical methods for the comprehensive analysis of oleogels-A review. *Polymers*, 13(1934), 1-23. <https://doi.org/10.3390/polym13121934>
- Righetti, M.C., Cinelli, P., Mallegni, N., Massa, C.A., Irakli, M. and Lazzeri, A. (2019). Effect of the addition of natural rice bran oil on the thermal, mechanical, morphological and viscoelastic properties of poly(Lactic Acid). *Sustainability (Switzerland)*, 11(10), 2783. <https://doi.org/10.3390/su11102783>
- Sahu, S., Ghosh, M. and Bhattacharyya, D.K. (2020). Utilization of unsaponifiable matter from rice bran oil fatty acid distillate for preparing an antioxidant-rich oleogel and evaluation of its properties. *Grasas y Aceites*, 71(1), a336. <https://doi.org/10.3989/gya.0938182>
- Silva, T.J., Barrera-Arellano, D., Ribeiro, A.P.B. (2021). Oleogel-based emulsions: Concepts, structuring agents, and applications in food. *Journal of Food Science*, 86(7), 2785-2801. <https://doi.org/10.1111/1750-3841.15788>
- Stahl, M.A., Buscato, M.H.M., Grimaldi, R., Cardoso, L.P. and Ribeiro, A.P.B. (2018). Structuration of lipid bases with fully hydrogenated crambe oil and sorbitan monostearate for obtaining zero-trans/low sat fats. *Food Research International*, 107, 61-72. <https://doi.org/10.1016/j.foodres.2018.02.012>
- Su, X., Lian, Z. and Yuan, Y. (2019). Study on the effect of the oil-water ratio on the rheological properties of hydroxyethyl cellulose (HEC). *Geofluids*, 2019, 7405702. <https://doi.org/10.1155/2019/7405702>
- Sun, P., Xia, B., Ni, Z.J., Wang, Y., Elam, E., Thakur, K., Ma, Y.L. and Wei, Z.J. (2021). Characterization of functional chocolate formulated using oleogels derived from β -sitosterol with γ -oryzanol/lecithin/stearic acid. *Food Chemistry*, 360, 130017. <https://doi.org/10.1016/j.foodchem.2021.130017>
- Widarta, I.W.R., Rukmini, A., Santoso, U., Supriyadi, and Raharjo, S. (2022). Optimization of oil-in-water emulsion capacity and stability of octenyl succinic anhydride-modified porang glucomannan (*Amorphophallus muelleri* Blume). *Heliyon*, 8(5), e09523. <https://doi.org/10.1016/j.heliyon.2022.e09523>
- Xu, D., Hao, J., Wang, Z., Liang, D., Wang, J., Ma, Y. and Zhang, M. (2021). Physicochemical properties, fatty acid compositions, bioactive compounds, antioxidant activity and thermal behavior of rice bran oil obtained with aqueous enzymatic extraction. *LWT-Food Science and Technology*, 149, 111817. <https://doi.org/10.1016/j.lwt.2021.1-8>
- Yang, S., Li, G., Saleh, A.S.M., Yang, H., Wang, N., Wang, P., Yue, X. and Xiao, Z. (2017). Functional characteristics of oleogel prepared from sunflower oil with β -sitosterol and stearic acid. *Journal of the American Oil Chemists' Society*, 94(9), 1153-1164. <https://doi.org/10.1007/s11746-017-3026-7>
- Zheng, J., Sun, D., Li, X., Liu, D., Li, C., Zheng, Y., Yue, X. and Shao, J.H. (2021). The effect of fatty acid chain length and saturation on the emulsification properties of pork myofibrillar proteins. *LWT-Food Science and Technology*, 139, 110242. <https://doi.org/10.1016/j.lwt.2020.110242>